DOI 10.1007/s11595-016-1495-4

AFM Analysis of TiN, TiAlN, and TiAlSiN Coatings Prepared by Cathodic Arc Ion Plating

WANG Wenchang[1], ZHANG Ling[2], KONG Dejun[2,3]*

(1.School of Petrochemical Engineering, Changzhou University, Changzhou 213164, China;2.College of Mechanical Engineering, Changzhou University, Changzhou 213164, China; 3.Jiangsu Key Laboratory of Materials Surface Science and Technology, Changzhou University, Changzhou 213164, China)

Abstract: The TiN, TiAlN, and TiAlSiN coatings were prepared on YT14 cutting tool surface with CAIP (cathode arc ion plating), the surface morphologies and phases were analyzed with FESEM (field emission scanning electron microscopy), and XRD (X-ray diffraction), respectively, and the coating parameters such as 3D surface micro-topography, grain size, surface height, hierarchy, profile height, and power spectral density, *etc*, were measured with AFM (atomic force microscope). The results show that the phases of TiN, TiAlN, and TiAlSiN coatings are TiN, TiN+TiAlN, TiN+Si_3N_4+TiAlN, respectively, while the surface roughness S_a of TiN, TiAlN, and TiAlSiN coatings is 75.3, 98.9, and 42.1 nm, respectively, and the roughness depth S_k is 209, 389, and 54 nm, respectively, the sequence of average grain sizes is TiAlN>TiN>TiAlSiN. The surface bearing index S_{bi} of TiN, TiAlN, and TiAlSiN coatings is 0.884, 1.01, and 0.37, respectively, and the sequence of surface bearing capability is TiAlN>TiN>TiAlSiN. At the lower wavelength (10^2-10^3 nm), the power spectral densities have a certain correlation, and the sequence of TiN>TiAlN>TiAlSiN, while the correlation is low at the higher wavelength (>10^3 nm).

Key words: TiN, TiAlN, and TiAlSiN coatings; AFM; 3D surface micro-topography; height analysis; power spectral density

1 Introduction

With the development of high efficiency and high precision machining, surface coating technology has been more widely used, as a chemical barrier and thermal barrier, the coating prevents the inter diffusion and chemical reaction between the tool and the workpiece, and the crescent wear is reduced. Comparing with the uncoated cutting tool, the coating may improve tool life by 3-5 times, meanwhile, the cutting speed increases by 20%-70%, and reduces the tool consumption cost by 20%-50%, and improves machining precision by 0.5-1 class[1]. As the first generation of cutting tool coating, the affinity between TiN coating and metal is small, the application range of cutting process is wide, the maximum working temperature can reach 500 ℃[2, 3]. TiAlN coating is formed by adding Al element to the TiN coating, which can increase the working temperature to 800 ℃, and Al_2O_3 formed by the high temperature cutting can effectively improve the wear resistance and the oxidation resistance[4,5]. TiAlSiN coating prepared by CAIP (cathodic arc ion plating) with the Ti/Si composite target formed by doping Ti target in pure Si can further improve the hardness, hot hardness and oxidation resistance at high temperature, the maximum working temperature can increase up to 1 100 ℃[6-8]. The material surface structures and properties are researched by using atomic interactions with atomic force microscope (AFM), of which the resolution can reach nanometer level[9], the 3D data of the surface morphology such as particle size, hierarchy, surface height and power spectral density, *etc*, can be obtained by calculation. At present, the relative researches are concentrated on cutting performance, wear-friction performance of high temperature, oxidation properties and corrosion resistance of TiN, TiAlN, and TiAlSiN coatings at home and abroad[10-12], while the surface

(Received: May 13, 2015; Accepted: July 4, 2016)

WANG Wenchang(王文昌): E-mail: kingsun717@126.com

*Corresponding author: KONG Dejun (孔德军): Ph D; E-mail: kong-dejun@163.com

Funded by the Jiangsu Province Science and Technology Support Program (Industry) (No.BE2014818)

microscopic morphologies of TiN, TiAlN, and TiAlSiN coatings have less been researched. The TiN, TiAlN, and TiAlSiN coatings were prepared on the surface of YT14 cutter with CAIP in this study, the surface morphologies, phases and microstructure evaluation parameters of TiN, TiAlN, and TiAlSiN coatings were firstly analyzed with FESEM, XRD and AFM, respectively, which provided a basis for the applications of TiN, TiAlN, and TiAlSiN coatings on cutting tool surface modification treatment.

2 Experimental

The substrate material was YT14 cutting tool material with the chemical compositions(wt%) as follows: WC 78, TiC 14, Co 8, the flexural strength≥ 2 200 N/cm^2, hardness≥82 HRA. After degreasing and sand blasting, the samples were cleaned with ultrasonic in acetone solution, dehydrated with anhydrous ethanol and dried in a constant temperature oven in turn. The coatings were plating on a PVT coating machine, the targets of Ti/Ti with the purity of 99.99%, Ti/Al with the purity of 99.99%, and Al/TiSi with the Ti purity of 80% and Si purity of 20% were adopted to prepare TiN, TiAlN, and TiAlSiN coatings, respectively, the technological parameters are shown as follows: vacuum degree of 3×10^{-4} Pa, furnace temperature of 500 ℃, reaction gas of N_2, plating time of 150 min, and protection gas of N_2. After annealing at 180 ℃ for 2 h, the samples were cleaned with acetone on a KQ2200DE CNC ultrasonic cleaner, obtaining the required samples. The morphologies and phases of TiN, TiAlN, and TiAlSiN coatings were analyzed with a SUPRA55 type FESEM and a D/max2500PC type XRD, respectively, and the surface morphology, grain size, hierarchy, surface height, profile height and power spectral density were analyzed with a CSPM5500 type AFM.

3 Results and discussion

3.1 Surface morphologies, EDS and XRD analysis

Figs.1 (a), (c) and (e) show the surface morphology of TiN, TiAlN, and TiAlSiN coatings, respectively, the sequence of surface quality was TiAlSiN>TiN >TiAlN according to the particle sizes

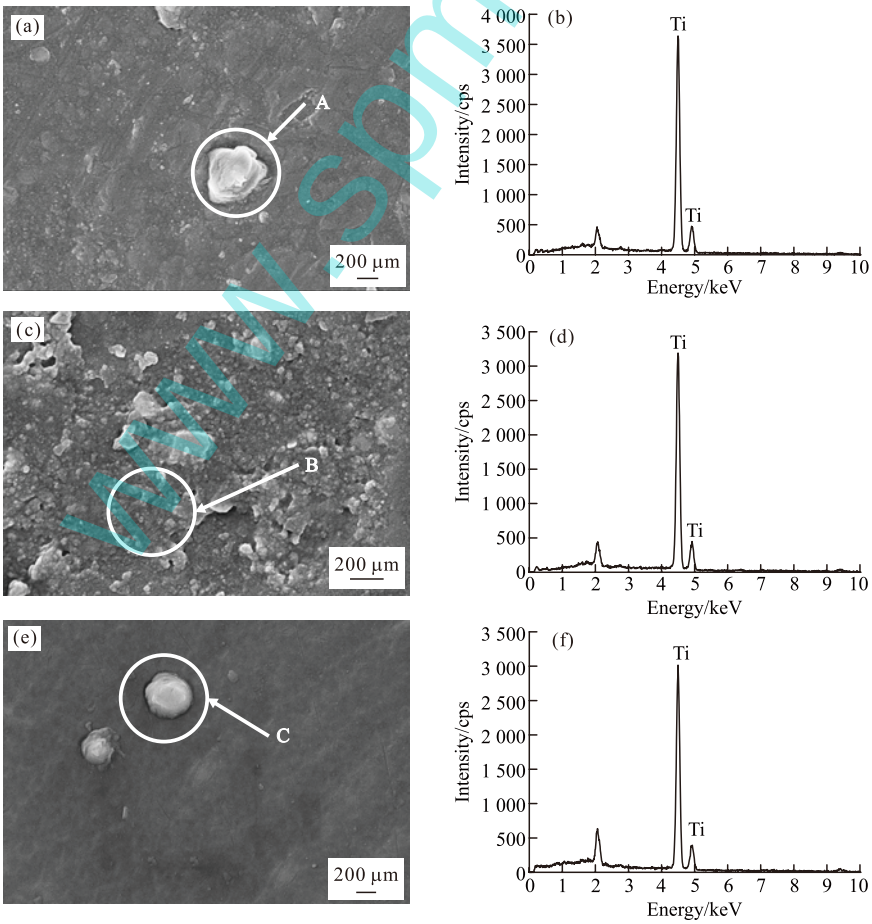

Fig.1 Surface morphologies and EDS analysis of TiN, TiAlN, and TiAlSiN coatings: (a) TiN coating morphology; (b) EDS analysis of A particle; (c) TiAlN coating morphology; (d) EDS analysis of B particle; (e) TiAlSiN coating morphology; (f) EDS analysis of C particle

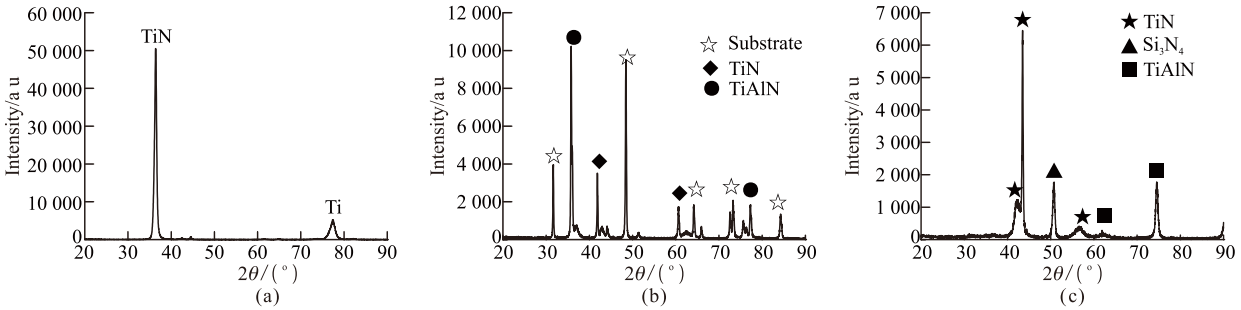

Fig.2 XRD analysis of TiN (a), TiAlN (b), and TiAlSiN (c) coatings

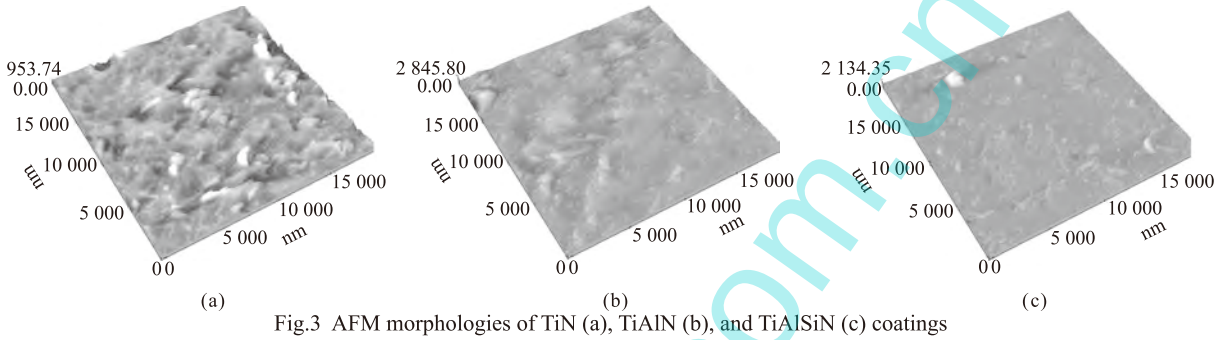

Fig.3 AFM morphologies of TiN (a), TiAlN (b), and TiAlSiN (c) coatings

on the coating surfaces. Some white particles of solidified materials appeared on the surfaces of three coatings, the EDS analyses indicated that the particles were composed of Ti element, as shown in Figs.1 (b), (d) and (f). This was because the metal ions were shot on the cathode surface during the deposition to cause partial metal melting and erupting, and combined into the small particles at high temperatures and attached to the coating surface, which had a certain effect on the coating surface roughness[13], the pits on the coating surfaces were due to the bombardment of polarized ions under high pressure[14].

Fig.2 shows the XRD analysis results of TiN, TiAlN, and TiAlSiN coatings, it can be seen that the composition of TiN coating was relatively single, mainly composed of TiN, there was a small number of non completely reacted Ti, the TiN phase of the (111) crystal plane had a preferred orientation, as shown in Fig.2 (a). The TiAlN coating was composed of TiN and TiAlN phases, as shown in Fig.2 (b), of which the phase of TiAlN was formed by Al replacing Ti of the TiN, therefore, the TiAlN phase also had a preferred orientation of (111) crystal plane. The substrate phases were also detected, which was due to the diffusion of the substrate elements into the coating surface in the process of deposition. The TiN, Si_3N_4, and TiAlN phases were detected in the TiAlSiN coating, of which the Si_3N_4 phase would generate SiO_2 at high temperature, which improved the wear resistance of the coating.

3.2 AFM morphologies

Fig.3 shows the AFM morphologies of TiN, TiAlN, and TiAlSiN coatings in the sampling range of 20 000 nm×20 000 nm. The surface roughness S_a of TiN, TiAlN, and TiAlSiN coatings was 75.3, 98.9 and 42.1 nm, respectively, as shown in Table 1, the corresponding square deviation of S_q was 107, 136, and 79.7 nm, respectively, the sequence was TiAlN>TiN>TiAlSiN, of which the surface roughness of TiAlSiN coating was the minimum, while that of TiAlN coating was the maximum. The surface roughness of TiAlN coating formed by adding Al element into TiN coating increased, which was because the Ti atoms of TiN were replaced by Al atoms that caused the molecular volume increase. While the Si element was added into the TiAlN coating, the surface roughness decreased, less than the surface roughness of TiN coating, which was because the adding of Si element was the role of grain refinement[7]. S_{sk} and S_{ku} were the characterizations of the convex peak shape on the coating surface, which was directly related to the surface contact mechanical behavior and had a direct influence on the friction and wear behaviors[15]. S_{sk} was a simple quantitative evaluation of the profile bearing length ratio curve shape, the surface skewness S_{sk} of TiN, TiAlN, and TiAlSiN coatings was 0.563, 0.365, and 4.05 nm, respectively, and the corresponding surface kurtosis S_{ku} was 5.95, 5.62, and 39.2 nm,

respectively, the S_{ku} values of three coatings were more than 3, as the leptokurtic curve, the sequence of the above two parameters was TiAlSiN>TiN>TiAlN. The values S_{sk} and S_{ku} were the smaller, the supporting performance of coating surface was better[9], it can be seen that the sequence of supporting performances was TiAlN>TiN>TiAlSiN. The profile maximum height value of S_y was the distance between profile peak line and valley line in the sampling range, S_z was the ten point height value, the sequence of the two parameters was TiAlN>TiAlSiN>TiN. The bigger the parameter value was, the greater the coating surface fluctuated, and also the worse the mechanical properties showed[10].

Table 1 Amplitude parameters of TiN, TiAlN, and TiAlSiN coatings

Parameters	TiN coating	TiAlN coating	TiAlSiN coating
Average roughness of S_a/nm	75.3	98.9	42.1
Mean square root of S_q/nm	107	136	79.7
Surface skewness of S_{sk}/nm	0.563	0.365	4.05
Surface kurtosis of S_{ku}/nm	5.95	5.62	39.2
Peak-peak of S_y/nm	854	1 960	1 730
Ten point height of S_z/nm	852	1 830	1 520

Table 2 Grain size parameters of TiN, TiAlN, and TiAlSiN coatings

Parameters	TiN coating	TiAlN coating	TiAlSiN coating
Total number of particles	833	791	963
Average area/nm^2	2.346×10^5	2.456×10^5	1.895×10^5
Average diameter/nm	546.7	559.2	491.2
Average height/nm	106.8	163.4	76.54
Maximum height/nm	433.5	904.9	1 046
Minimum height/nm	6.8	15.94	18.24

Fig.4 shows the particle scale distribution of TiN, TiAlN, and TiAlSiN coating surfaces. The particle scale parameters of three coatings are shown in Table 2, the particle number of TiN, TiAlN, and TiAlSiN coatings was 833, 791, and 963, respectively, the corresponding particle area was 2.346×10^5, 2.456×10^5, and 1.895×10^5 nm^2, respectively, the sequence of particle scale was TiAlN>TiN>TiAlSiN. According to the Hall-Petch equation, it was indicated that the smaller grains had the higher hardness, which was beneficial to reducing the friction coefficient and wear extent.

3.3 Height analysis

Fig.5 shows the surface height distributions of TiN, TiAlN, and TiAlSiN coatings. The sequence of high dispersion degree of three coatings was TiN>TiAlN>TiAlSiN, respectively. The height distribution of the TiN coating was most close to the Gauss distribution, of which supporting capacity was the best, the surface distribution was more dispersed, the surface supporting length rate on the surface profile increased, the convex of coating surface was slower, which was helpful to improve the supporting capacity and wear resistance of the coatings, and the sequence of the supporting capacity of three coatings was TiN > TiAlN >TiAlSiN.

Fig.6 shows the hierarchy analysis chart of three coatings, which was another statistical form of surface height value, the three curves were smooth, and all the courses were processed as the rule, without impact process[16].

The section length of 15 000 nm were selected to analyze the coating, the obtained profiles are showed

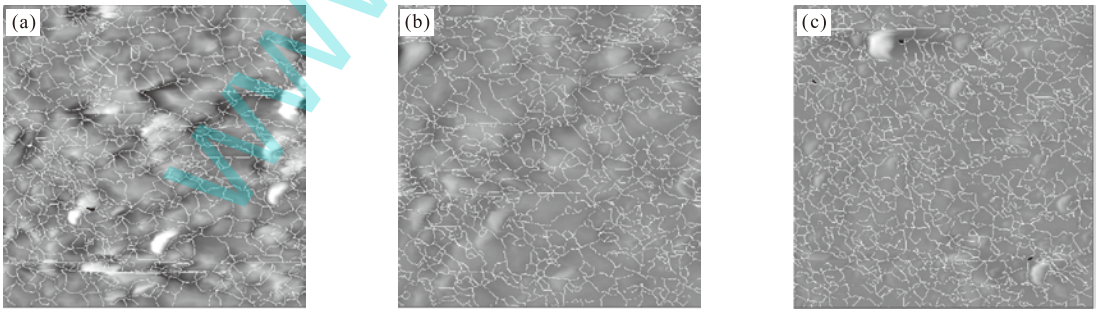

Fig.4 Grain size analysis of TiN (a), TiAlN (b), and TiAlSiN (c) coating surfaces

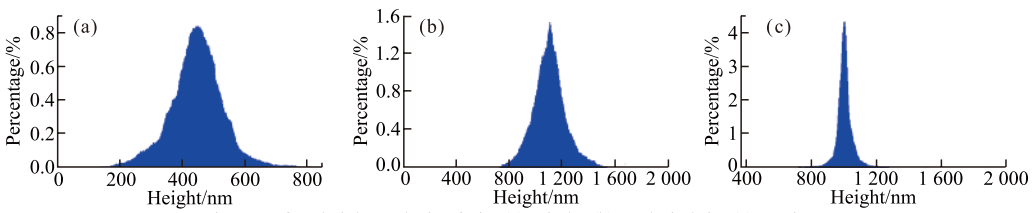

Fig.5 Surface height analysis of TiN (a), TiAlN (b), and TiAlSiN (c) coatings

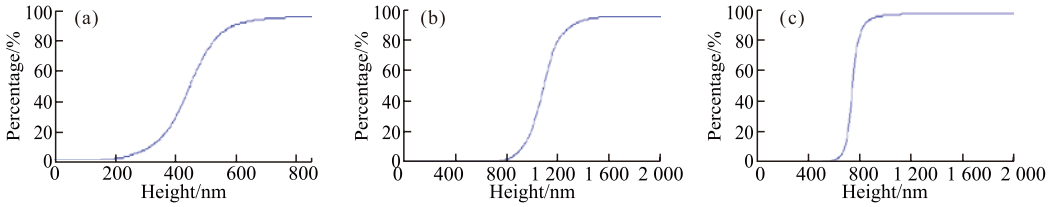

Fig.6 Surface hierarchy analysis of TiN (a), TiAlN (b), and TiAlSiN (c) coatings

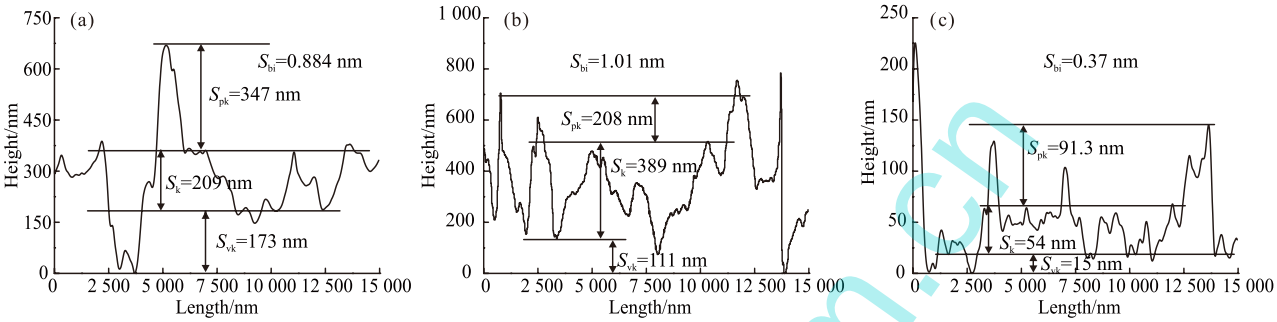

Fig.7 Profile height analysis of TiN (a), TiAlN (b)and TiAlSiN (c) coatings

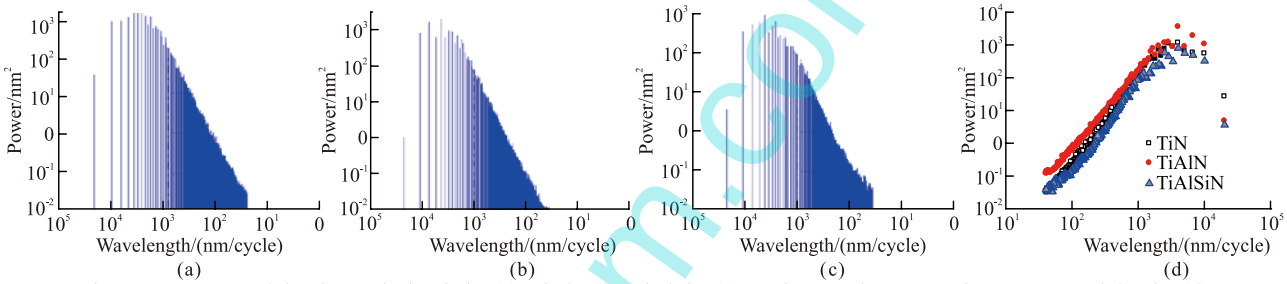

Fig.8 Power spectral density analysis of TiN (a), TiAlN (b), TiAlSiN (c) coatings, and contrast of power spectral density (d)

in Fig.7, where S_{pk} was the reduced wave crest height, the representing peak was contact of friction pairs on initial wear, this part would usually be worn out in the running-in stage. S_k was the core roughness depth, during the normal wear the part was mainly worn by load, which affected the lubricant and wear debris, mainly relating to the performance of removing debris[17]. S_{vk} was the reduced trough depth, bearing after normal wear, which had little effect on the wear mechanism of the coating. Fig.7 (a) shows the profile height analysis of TiN coating, including S_{pk} of 347 nm, S_k of 209 nm and S_{vk} of 173 nm, of which surface bearing coefficient S_{bi} was 0.884. Fig.7 (b) shows the profile height analysis of TiAlN coating, including S_{pk} of 208 nm, S_k of 389 nm, S_{vk} of 111 nm, of which the surface bearing coefficient S_{bi} was 1.01. Fig.7 (c) shows the profile height analysis of TiAlSiN coating, including S_{pk} of 91.3 nm, Sk of 54 nm, S_{vk} of 15 nm, of which surface bearing coefficient S_{bi} was 0.37. From the above analyses, the sequence of S_k was TiAlN>TiN>TiAlSiN, the surface bearing coefficient S_{bi} was also the same as that of S_k, and the sequence of surface bearing properties of TiN, TiAlN, and TiAlSiN coatings was TiAlN>TiN>TiAlSiN, which was consistent with the results of the height analysis.

3.4 Power spectrum density

Table 3 Power spectral density parameters of TiN, TiAlN, TiAlSiN coatings

Parameters	TiN coating	TiAlN coating	TiAlSiN coating
Total power	6.35×10^3	1.85×10^4	1.14×10^4
Mean square root/nm	79.7	136	107
Cursor's power/nm^2	4.95×10^3	1.46×10^4	9.49×10^3

Fig.8 shows the distributions of power spectral density of three coatings, the corresponding parameters are shown in Table 3, the total power of TiN, TiAlN, and TiAlSiN coatings was 6.38×10^3, 1.85×10^4, and 1.14×10^4 nm^3 within the scope of assessment, respectively, and the corresponding surface wavelength distribution was 60-3×10^4, 80-6×10^4, and 70-4×10^4 nm, respectively, as shown in Figs.8 (a)-(c). Therefore, the wavelengths of three coatings surfaces were not concentrated on one place, when the wavelength changed at the horizontal axis, the power spectrum peak appeared no obvious, which indicated that the

morphologies of the coating surfaces were caused by random factors in the course of processing, there were no fixed rules, as for anisotropic. Fig.8 (d) shows the contrast of power spectral density of three coatings, near the low wavelength of 10^2-10^3 nm, the power spectrum density of three coatings had certain correlation, while at higher wavelength >10^3 nm, the correlation was low[18,19].

Selecting the linear part of the data (wavelength λ<103.2), for fitting straight line, three equations can be obtained as follows:

$$y_1=2.587\ 8x-5.753\ 3 \quad (1)$$

$$y_2=2.331\ 2x-4.845\ 9 \quad (2)$$

$$y_3=2.466\ 3x-5.676\ 6 \quad (3)$$

where $y=\log P$, $x=\log\lambda$.

For the low wavelength, the coating power spectral density P and wavelength λ had the following relationships.

For the TiN coating

$$P=10^{2.587\ 8\log\lambda-5.753\ 3} \quad (4)$$

For the TiAlN coating

$$P=10^{2.331\ 2\log\lambda-4.845\ 9} \quad (5)$$

For the TiAlSiN coating

$$P=10^{2.466\ 3\log\lambda-5.676\ 6} \quad (6)$$

From Eqs.(4)-(6), it can be seen that at the same low wavelength, the sequence of power spectrum density was TiN>TiAlN>TiAlSiN.

4 Conclusions

a) The TiN, TiAlN and TiAlSiN coatings are mainly composed of TiN, TiAlN+TiN, TiN+Si_3N_4+TiAlN phases, respectively, and the main composition of white particles on the TiN, TiAlN and TiAlSiN coating surfaces is Ti element.

b) The sequence of surface quality of the TiN, TiAlN, and TiAlSiN coating is TiAlSiN>TiN>TiAlN, the sequence of S_{sk} and S_{ku} size is TiAlSiN>TiN>TiAlN, and the sequence of S_k and S_{bi} size is TiAlN>TiN>TiAlSiN, while the sequence of surface bearing performance is TiAlN>TiN>TiAlSiN.

c) The sequence of power spectral density of the TiN, TiAlN, and TiAlSiN coatings at low wavelength (10^2-10^3 nm) is TiN>TiAlN>TiAlSiN, while at higher wavelength (>10^3 nm) the correlation is low, the surface wavelength has not formed a regional focus, and the power spectrum diagram has no obvious peak appeared, as anisotropy.

References

[1] Wu Wenji, Xin Zhijie. *Metal Cutting Principle and Tool*[M]. Beijing: National Defence Industry Press, 2009

[2] Ying Chen, Nie Xueyuan. Study on Fatigue and Wear Behaviors of a TiN Coating Using an Inclined Impact-sliding Test[J]. *Surface & Coatings Technology*, 2011, 206: 1 977-1 982

[3] Zhu Changjun, Chen Kanghua, Wang Shequan, *et al*. Effects of Gradient Substrate Structure on Oxidation Resistance of TiN Coated Cemented Carbide[J]. *Journal of Central South University (Science and Technology)*, 2011, 42 (10): 2 984-2 988

[4] Fox-Rabinovich G S, Endrino J L, Beake B D, *et al*. Effect of Temperature of Annealing below 900 ℃ on Structure, Properties and Tool Life of an AlTiN Coating under Various Cutting Conditions[J]. *Surface & Coatings Technology*, 2008, 202: 2 985-2 992

[5] Feng Changjie, Hu Shuilian, Jiang Yuanfei, *et al*. Effect of Shielded Plate Size on the Microstructure and Tribological Properties of TiAlN Coating Prepared by Arc ion Plating[J]. *Tribology*, 2013, 33 (6): 606-613

[6] Kong Dejun, Fu Guizhong, Zhang Lei, *et al*. Microstructures and Properties of TiAlSiN Coating Prepared by Cathodic Arc ion Plating[J]. *Journal of Central South University (Science and Technology)*, 2014, 44 (9): 3 645-3 651

[7] Miletic A, Panjan P, Skoric B, *et al*. Microstructure and Mechanical Properties of Nanostructured Ti-Al-Si-N Coatings Deposited by Magnetron Sputtering[J]. *Surface & Coatings Technology*, 2014, 241: 105-111

[8] Chang Yinyu, Yang Shunjan, Wu Weite, *et al*. Mechanical Properties of Gradient and Multilayered TiAlSiN Hard Coatings [J]. *Thin Solid Films*, 2009, 517 (17): 4 934-4 937

[9] Joost Te Riet, Allard J Katan, Christian Rankl, *et al*. Interlaboratory Round Robin on Cantilever Calibration for AFM Force Spectroscopy [J]. *Ultramicroscopy*, 2011, 111 (12): 1 659-1 669

[10] Nguyen Dang Nam, Mahesh, Nguyen Tran Hung. Corrosion Behavior of TiN, TiAlN, TiAlSiN-coated 316L Stainless Steel in Simulated Proton Exchange Membrane Fuel Cell Environment[J]. *Journal of Power Sources*, 2014, 268: 240-245

[11] Wang Shequan, Chen Kanghua, Xu Yinchao, *et al*. Effect of Substrate Gradient Structure on Mechanical and Getting Properties of TiN Coated Cemented Carbide[J]. *The Chinese Journal of Nonferrous Metals*, 2011, 21 (4): 804-809

[12] Shum P W, Zhou Z F, Li K Y. Friction and Wear Reduction of Hard TiAlSiN Coatings by an Integrated Approach of Laser Surface Texturing and High-energy Ion Implantation[J]. *Surface & Coatings Technology*, 2014, 259: 136-140

[13] Chen Meiyan, Tong Honghui, Shen Liru, *et al*. High Adhesion TiN Film Deposition on 15-5PH Steel Substrate by the Multi-arc ion Plating Technique[J]. *Journal of Functional Materials*, 2012, 43 (13): 1 802-1 805

[14] Wei Yongqiang, Li Chunwei, Gong Chunzhi, *et al*. Microstructure and Mechanical Properties of TiN/TiAlN Multilayer Coatings Deposited by Arc ion Plating with Separate Targets[J]. *Transactions of Nonferrous Metals Society of China*, 2011, 21 (5): 1 068-1 073

[15] Ge Shirong, Zhu Hua. *Fractal of Tribology*[M]. Beijing: Machinery Industry Press, 2005

[16] Fu Guizhong, Kong Dejun, Zhang Lei, *et al*. Microstructures of AlCrN Coatings Synthesized by Cathodic Arc Ion Plating[J]. *Chinese Journal of Vacuum Science and Technology*, 2014, 34 (5): 477-482

[17] Pinar Demircioglu. Surface Topographical Evalution of Coated Cutting Tools with Different Coating Technologies[J]. *Measurement*, 2014, 47: 893-902

[19] Chan Su Han, Bhaskar Chandra Mohanty, Hong Rak Choi, *et al*. Surface Scaling Evolution and Dielectric Properties of Sputter-deposited Low loss Mg_2SiO_4 Thin Films[J]. *Surface & Coatings Technology*, 2013, 231: 229-233